RSC Advances

PAPER

View Article Online
View Journal | View Issue

Cite this: *RSC Adv.*, 2020, **10**, 44672

Attenuation of Cr/Pb in bauxite leachates by bentonite–polymer composite geosynthetic clay liners

Qin Li, Daoping Peng,* Zheng Wu and Tao Huang

Three commercially available bentonite–polymer composite geosynthetic clay liners (BPC GCLs) were selected for hydraulic conductivity testing, respectively permeated by two types of bauxite leachates with high alkalinity (pH > 12) and high ionic strength (620.3 mM). The influence of BPC GCLs on the attenuation behavior of Cr/Pb in the bauxite leachates was analyzed. The BPC GCLs with a low hydraulic conductivity ($k < 10^{-10}$ m s^{-1}) retard the migration of Cr and Pb and the Cr had a higher mobility than Pb in the BPC GCLs. Scanning electron microscope (SEM) microstructure analysis showed that the migration and attenuation behavior of Cr/Pb mainly depended on the chemical properties of the leachates, polymer content and the microstructure of the polymer. Higher attenuation of heavy metals was obtained with bauxite leachates having higher ionic strength. Sufficient polymer content is needed to ensure BPC GCLs have adequately low hydraulic conductivity to suppress attenuation of heavy metals. The gelatinous structure associated with hydrated linear or crosslinked polymer diminishes when the polymer in a BPC is in contact with bauxite leachates. Compromising the hydrogel structure promotes polymer elution and leaves pore space open, resulting in attenuation of heavy metals.

Received 13th August 2020
Accepted 3rd December 2020

DOI: 10.1039/d0ra06921c

rsc.li/rsc-advances

1. Introduction

With the continuous acceleration of the industrialization process, the treatment and disposal of solid waste has become an urgent problem to be solved. Red mud is a kind of very fine particle strongly alkaline solid waste produced in the process of alumina production.[1,2] Approximately 1–1.5 tons of red mud are generated for every 1 ton of alumina produced.[3] Bauxite leachates exuded in a stacking process have high pH (>14 in some cases) and high ionic strength (>1 M in some cases).[4–6] Bauxite leachates not only have strong alkalinity but also dissolve a large amount of elements containing a large amount of K, Na, Ca, Mg, Al, OH^-, F^-, Cl^-, SO_4^{2-}, *etc.*[7–10] The pH value is as high as 12 or 13, and large amounts of heavy metal elements are dissolved, and arsenic (As), lead (Pb), zinc (Zn), copper (Cu), nickel (Ni), chromium (Cr), and vanadium (V),[11–14] usually are at concentrations beyond groundwater quality standards in the United States and China.[6] For example, the concentration of As and Cr in bauxite leachates is 2 to 200 times higher than the maximum contaminant level (MCL) issued by the US Environmental Protection Agency.[6] Therefore, bauxite leachates may contaminate groundwater if it is not stored in a properly designed and managed disposal facility.

Geosynthetic clay liners (GCLs) with strong adsorption and low permeability have been widely used in red mud storage according to the environmental protection and anti-seepage requirements.[15–18] GCLs are geosynthetic materials made of two layers of geotextile (woven or non-woven) with a layer of 5–10 mm thick natural sodium-based bentonite, which are knitted and reinforced.[19,20] The main component of sodium-based bentonite is sodium-based montmorillonite,[21] which produces osmotic expansion through strong water absorption of sodium ions, reduces seepage pores and increases curvature.[22,23] However, extreme pH conditions, cation exchange, and high ionic strength solutions could cause sodium-based montmorillonite to lose its permeability.[24,25]

In order to improve the chemical permeability of conventional sodium bentonite GCLs, bentonite–polymer composite GCLs (BPC GCLs) have been developed in recent years.[26–28] The research of hyperbranched poly(amidoamine) (PAMAM) as a continuous phase using aqueous dispersion method showed that intercalation of PAMAM took place in pre-expanded kaolinite to give exfoliated nanocomposite.[29] The modified montmorillonite by the preparation of poly (methylmethacrylate) nanocomposites with basal distance 1.95 nm exhibited better thermal stability and revealed tremendous affinity for removing pesticides from aquatic solutions.[30] The prepared of polyaniline/montmorillonite nanocomposites by intercalating the emulsion of aniline monomer with treated organically layers using ammonium peroxydisulfate as an initiator showed an enhancement in the conductivity values.[31]

The modified bentonite GCLs use polymer (such as sodium carboxymethyl cellulose) as an additive to modify sodium bentonite which make it resistant to harsh chemical

School of Geosciences and Environmental Engineering, Southwest Jiaotong University, Chengdu, China. E-mail: pdp0330@swjtu.cn

environments.[32,33] A large number of studies have shown the characterized behaviour of BPC GCLs to coal combustion product leachate (pH = 8.5, I = 39.5 mM), trona leachate (pH = 11, I = 1.05 M) and bauxite leachate (pH = 13, I = 2.35 M), but the attenuation of heavy metals has received little attention.[15,28] The attenuation of heavy metals in BPC GCLs is mainly attributed to the adsorption on clays, especially under different environmental conditions.[34] Studies on the migration of zinc oxide nanoparticles (nZnO) in geosynthetic clay liners (GCLs) have found that the migration of metals has a great relationship with osmotic pressure. As the pressure increases, the pores of the GCL are compressed and the attenuation of nZnO is greatly reduced.[35] Through long-term prediction research on the reduction of heavy metals by GCLs, it is found that GCLs can effectively delay the breakthrough times of heavy metals, especially the attenuation of heavy metals Fe and Mn adsorbed on the bentonite showed regularity.[36] However, the attenuation mechanism, especially the material analysis method using microscopic imaging, has not been thoroughly understood.

The purpose of this study is to explore the mechanism that control the attenuation of the heavy metals of BPC GCLs. Hydraulic conductivity tests were conducted on commercially available BPC GCLs using two characteristic Chinese bauxite leachates and the attenuation of different heavy metals is evaluated. Micro-scale image analysis of specimens obtained by scanning electron microscopy (SEM) was used to understand mechanisms controlling the attenuation of the heavy metals permeated with bauxite leachates.

2. Materials and methods

2.1 Bentonite–polymer composite geosynthetic clay liners (BPC GCLs)

In this study three BPC GCLs which are commercially available in China were employed. For each GCL, the BPC mixture containing dry mixing granular sodium bentonite with granular proprietary polymers was encased between woven and nonwoven geotextiles bonded by needle-punching. The main component of these polymers is anionic polyacylamide (PAM). PAM is composed of polymer chains which have hydrophilic functional groups, bonded by hydrogen bonding to form a hydrogel.[37] These BPC GCLs are labeled as CP6.5, CP7.5, CP10.8, with the numerical suffix representing the polymer content in % dry mass.

Bentonite mineralogy, physical properties, and polymer content of the GCLs are showed in Table 1. Each BPC GCL comprised sand-sized bentonite granules with a median particle size (D50) between 0.7 mm and 0.9 mm. Clay minerals and bulk minerals on the bentonite were quantified using Quantitative X-ray diffraction (XRD).[38] The bentonite contained 67% to 85% montmorillonite, and measurable quartz, feldspar, illite, calcite, kaolinite, potassium feldspar. Polymer content of BPC GCLs was measured based on loss on ignition (LOI).[39]

2.2 Bauxite leachates and chemical analysis

In this study, two typical bauxite leachates were used from two red mud management facilities in two provinces of China: GX (Pingguo County, Guangxi) and SD (Zibo, Shandong). Two characteristic of bauxite leachates were employed for testing: (1) SD (I = 620.3 mM, RMD = 2.6 $M^{1/2}$) which containing the highest ionic strength, represented the worst-case scenario that might be encountered in a red mud impoundment in China, and (2) GX (I = 224.5 mM, RMD = 0.03 $M^{1/2}$) which containing an moderate ionic strength and lower RMD, represented the general bauxite

Table 2 Chemical parameters and concentrations of major elements, anions, and heavy metals of bauxite leachates

Leachate samples	GX	SD
Chemical parameters		
pH	12.1	12.6
EC @ 25 °C (S m^{-1})	0.97	5.11
ORP (mV)	−46.0	−110.0
Ionic strength (mM)	224.5	620.3
RMD ($M^{1/2}$)	0.03	2.6
Major elements and anions		
Al (mg L^{-1})	1095.5	745.5
Ca (mg L^{-1})	88.9	57.1
Na (mg L^{-1})	3506.0	10 650.0
Mg (mg L^{-1})	15.0	10.5
K (mg L^{-1})	239.3	81.8
Si (mg L^{-1})	41.7	89.9
Cl^- (mg L^{-1})	877.1	6490.5
F^- (mg L^{-1})	49.8	121.8
SO_4^{2-} (mg L^{-1})	741.7	7453.3
Heavy metals		
Cr (mg L^{-1})	0.1	5.9
Pb (mg L^{-1})	0.3	1.1

Table 1 Properties of bentonite–polymer composite geosynthetic clay liners used in this study

	Geosynthetic clay liner		
Property	CP6.5	CP7.5	CP10.8
Bentonite mass per unit area (kg m^{-2})	3.6	3.7	3.6
Initial thickness (mm)	6.4–7.4	5.9–6.7	6.5–7.3
Initial water content (%)	4.4	4.8	5.6
Median granule size (mm)	0.8	0.7	0.9
Montmorillonite content (%)	76	67	85
Loss on ignition (%)	8.0 ± 0.5	9.0 ± 0.3	12.2 ± 0.4
Polymer content (%)	6.5 ± 0.5	7.5 ± 0.3	10.8 ± 0.4

leachates. Chemical parameters, including pH, EC, ORP, ionic strength, and relative abundance of monovalent and polyvalent cations (RMD) of the two bauxite leachates are showed in Table 2.

The pH, EC, and oxidation–reduction potential (ORP) of bauxite leachates were evaluated with accumet XL50 bench-top meters (Fisher Scientific, Hanover Park, IL). The bauxite leachates are hyperalkaline, with pH ranging from 11.3 to 13.2. The ionic strength ranges from 77.3 mM to 620.3 mM. EC of the bauxite leachates ranges from 0.44 to 5.11 S m^{-1} at 25 °C. The ORP ranges from −110.0 to −63.0 mV which indicated a reducing condition.

The concentrations of major elements (Na, K, Ca, Mg, Al, and Si) and heavy metals (Cr and Pb) of the bauxite leachates, the influent, and the effluent were evaluated by inductively coupled plasma mass spectrometry (ICP-MS, Agilent Technologies 700 Series, Santa Clara, CA, USA). The anions of the bauxite leachates, including chloride (Cl^-), fluoride (F^-), and sulfate (SO_4^{2-}), were conducted by ion chromatography (IC, Shimadzu HIC-SP, Kyoto, Japan).The major elements of the bauxite leachates are Al (152–1090 mg L^{-1}) and Na (1200–41 300 mg L^{-1}) and the major anions are Cl^- (150–6590 mg L^{-1}) and SO_4^{2-} (162–7450 mg L^{-1}).

2.3 Hydraulic conductivity tests

Hydraulic conductivity tests were examined following the falling headwater-constant tailwater method and the specimens of BPC GCLs with a diameter of 150 mm were installed in the flexible-wall permeameters.[40] Bauxite leachates GX and SD were employed as permeant liquids to represent the worst-case chemistry (SD) and the moderate chemistry (GX). ASTM Type II DI water as permeant liquid was conducted as control tests.

The specimens of BPC GCLs were hydrated with permeant liquids for 48 h in the flexible-wall permeameters which were assembled at an effective stress of 20 kPa and hydraulic gradient of 0. Hydraulic conductivity tests continued until termination criteria was reached. The hydraulic equilibrium and chemical equilibrium of termination criteria generally were satisfied between BPC GCLs and permeant liquids:[41,42] (1) the ratio of incremental outflow to inflow (Q_{out}/Q_{in}) was within 1 ± 0.25, (2) the pH and electrical conductivity (EC) of the effluent were within 10% of the influent, pH_{out}/pH_{in} and EC_{out}/EC_{in} were within 1 ± 0.1 (3) the concentrations of major cations (*i.e.*, Na^+, K^+, Ca^{2+}, and Mg^{2+}) of the effluent were within 10% of the influent.

2.4 Swell index

Two bauxite leachates and ASTM Type II DI water were used as the hydrating liquid. The swell index of bentonite from each BPC GCLs was evaluated. The bentonite from each BPC GCLs was passed the No. 200 US standard sieve (0.075 mm) after grounding with a mortar and pestle to and oven-dried for 24 hours at 105 ± 5 °C until constant mass. The 2 g of ground bentonite was added to the cylinder in 0.1 g increments and the graduated cylinder was filled to 100 mL. The graduated cylinder was let sit for 24 h and the swell index was recorded.

2.5 Scanning electron microscope (SEM)

The microscale state of the bentonite which contained pore-scale structure, polymer structure and clay–polymer interactions in the BPC GCLs was analyzed by scanning electron microscope (SEM) with energy-dispersive X-ray spectroscopy (EDS). The specimens of BPC GCLs were prepared by freeze-drying with liquid nitrogen (−90 °C) under 20 kPa vacuum (Vacuum Freeze Drier, LGJ-10, Beijing, China). The original microstructure of the hydrated condition could be retained and stable by freeze-dry system. The freeze-dried specimens 2 mm-thick were cut using a surgical knife and then coated with gold by sputtering (Denton Vacuum Desk II, Moorestown, NJ, USA). SEM images of freeze-dried specimens were obtained using an FEI Nova Nano SEM (SEM450, Hillsboro, OR, USA) using a 3 keV electron beam and a conventional secondary electron detector.

3. Results and discussion

3.1 Attenuation of Cr/Pb in bauxite leachates by BPC GCLs

Hydraulic conductivity, swell index, and the cumulative inflow of breakthrough Cr/Pb to DI water and bauxite leachates are shown in Table 3. In this study, all hydraulic conductivity tests fulfilled the hydraulic equilibrium and chemical equilibrium criteria. The ratio of inflow and effluent concentrations for Cr and Pb (*i.e.*, C_{Cr}/C_{Cro} and C_{Pb}/C_{Pbo}) in the hydraulic conductivity tests to the SD and GX bauxite leachates is shown in Fig. 1. The concentrations of Cr (Pb) in the SD and GX bauxite leachates are 5.9 (1.1) and 0.1 (0.3) mg L^{-1}, respectively. The breakthrough of heavy metal is identified when the concentration in the effluent reaches its initial value, *i.e.*, $C/C_o = 1$, where C is the effluent concentration and C_o is the initial concentration.[36]

It can be clearly seen from Table 3 and Fig. 1 that as the number of polymers increases, the hydraulic conductivity gradually decreases and the breakthrough time of Cr/Pb is delayed accordingly. Moreover, the breakthrough time of SD bauxite leachates with the highest ionic strength was significantly earlier than that of GX bauxite leachates with low ionic strength. The ratios of C_{Cr}/C_{Cro} and C_{Pb}/C_{Pbo} increase systematically as the permeation continuous. The Cr breakthrough (*i.e.*, $C_{Cr}/C_{Cro} = 1$) for the CP6.5 GCL occurred at a 1500 mL cumulative inflow when permeated with the SD bauxite leachates. The breakthrough of Cr is likely due to the high hydraulic conductivity of the CP6.5 GCL to SD (5.0×10^{-9} m s^{-1}), and the migration of Cr is likely controlled from advection. In the early stage, the breakthroughs of Cr and Pb for the tests with low hydraulic conductivities (<10^{-10} m s^{-1}) were not evident during the current testing period (>1000 mL cumulative inflow or >10 PVFs). After a long period of testing (cumulative flow > 2000 mL or >20 PVFs), the breakthrough of Cr and Pb in the test of low hydraulic conductivity (<10^{-10} m s^{-1}) becomes obvious and the maximum C_{Cr}/C_{Cro} reaches approximately 1. Comparing the C/C_o for Cr and Pb, the Cr has a higher mobility than Pb, which is likely due to the formation of the highly soluble oxyanion (*i.e.*, CrO_4^{2-}) when under alkaline conditions.

3.2 Effect of bentonite in BPC GCLs on attenuation of Cr/Pb

The effect of bentonite in BPC GCLs on attenuation of heavy metals is mainly reflected in two points: adsorption

Table 3 Summary of hydraulic conductivity, swell index and the cumulative inflow of breakthrough Cr/Pb of BPC GCLs to DI water and bauxite leachates

GCL	Permeant liquid	Hydraulic conductivity (m s^{-1})	Swell index (mL/2 g)	C_{Cr}/C_{Cro} = 1 (mL)	C_{Pb}/C_{Pbo} = 1 (mL)
CP 6.5	DI water	1.7×10^{-13}	29.0	—	—
	GX	3.1×10^{-11}	18.0	2380	2100
	SD	5.0×10^{-9}	8.2	1500	1660
CP 7.5	DI water	3.3×10^{-12}	28.0	—	—
	GX	7.2×10^{-11}	16.0	2520	2430
	SD	6.7×10^{-11}	6.5	1800	1880
CP 10.8	DI water	9.6×10^{-12}	28.0	—	—
	GX	3.2×10^{-11}	17.0	2700	2560
	SD	6.6×10^{-12}	5.9	1900	2140

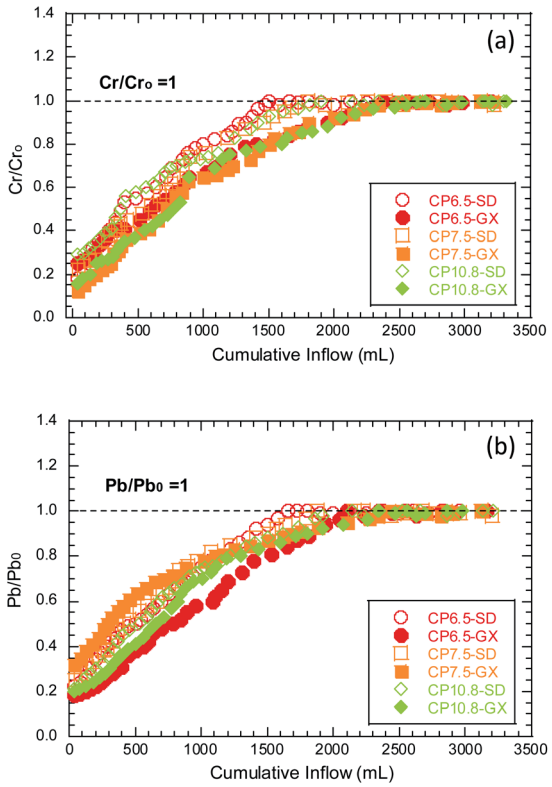

Fig. 1 The ratio of the inflow and effluent concentrations for (a) Cr (*i.e.*, C_{Cr}/C_{Cro}) and (b) Pb (*i.e.*, C_{Pb}/C_{Pbo}) in the hydraulic conductivity tests to the SD and GX bauxite leachates.

performance and osmotic expansion performance. The adsorption performance is mainly due to the ion exchange property of bentonite. Bentonite is a non-metallic mineral with montmorillonite as the main mineral component. The montmorillonite structure is a 2 : 1 type crystal structure composed of two silica tetrahedrons and a layer of aluminum octahedrons. There are certain cations in the layered structure, such as Cu, Mg, Na, K, *etc.* The interaction of these cations with the smectite unit cell is very unstable and easily exchanged by other cations, so it has good ion exchange. When sodium-based bentonite containing cation Na^+ is exposed to bauxite leachates with high ion concentrations or a large lot of divalent cations, Na^+ undergoes ion exchange with the heavy metal cation in the bauxite leachates. This is consistent with the rapid decrease in the concentration of heavy metals at the beginning in Fig. 1. The gradual upward trend in the concentration of heavy metals in the latter part of the tests is due to the reversible ion exchange effect, and the desorption gradually occurs with the long-term soaking of the bauxite leachates.

The osmotic expansion of bentonite in BPC GCLs is another major factor contributing to the attenuation of heavy metals. Swell index of the bentonite BPC GCLs is shown in Fig. 2 as a function of bauxite leachates. The attenuation of heavy metals is closely related to the swell index of bentonite, which indicates that the osmotic mechanism of bentonite controls the attenuation of heavy metals. As the swell index increases, the hydraulic conductivity becomes smaller, which lead to smaller penetration and slower attenuation of heavy metals. For example, the swell index for the CP6.5 of BPC GCLs decreases with increasing bauxite leachates concentration (Table 3) from approximately 29 mL = 2 g in DI water to 8.2 mL = 2 g in SD bauxite leachates and correspondingly the hydraulic conductivity is 1.7×10^{-13} m s^{-1} to DI water and 1.7×10^{-9} m s^{-1} for SD bauxite leachates with higher ionic strength. The time of breakthrough Cr increased from 1500 mL to 2380 mL with increasing the swell index in SD and GX bauxite leachates. Similarly, the time of

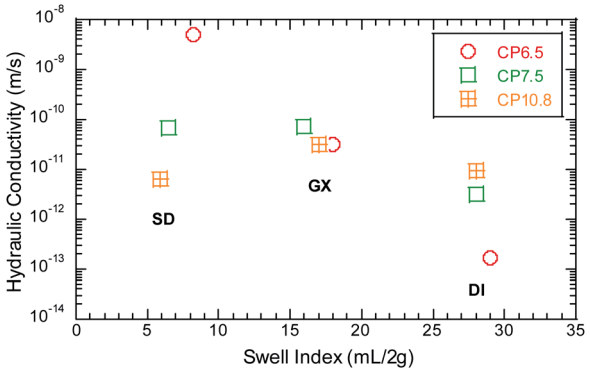

Fig. 2 Hydraulic conductivity *vs.* swell index for CP6.5, CP7.5 and CP10.8.

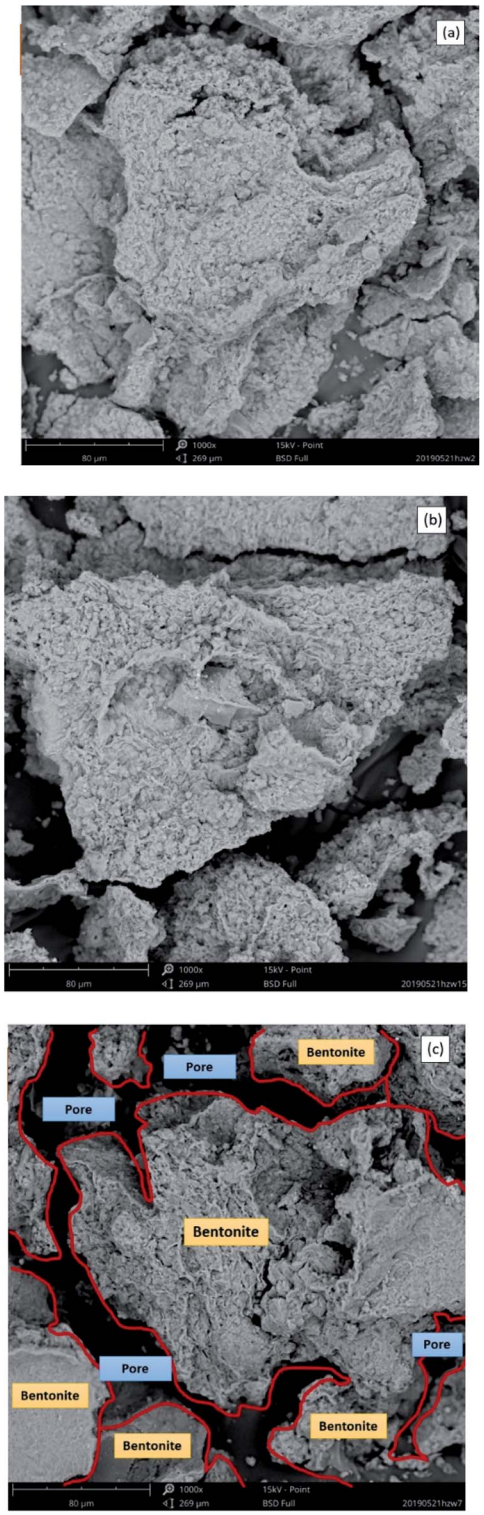

Fig. 3 SEM images of bentonite permeated with DI water and bauxite leachates. (a) SEM images of bentonite permeated with DI water. (b) SEM images of bentonite permeated with GX bauxite leachates. (c) SEM images of bentonite permeated with SD bauxite leachates.

breakthrough Pb was earlier for SD bauxite leachates with higher ionic strength than GX bauxite leachates.

SEM images permeated with DI water and bauxite leachates illustrate how osmotic expansion of bentonite affects the attenuation of heavy metals (Fig. 3). Fig. 3(a) shows the microstructure of the SEM about the sodium-based bentonite permeated with DI water. The montmorillonite mineral layer in the bentonite could occur osmotic expansion and absorb a large amount of water, which result very low hydraulic conductivity of bentonite. The osmotic expansion reduces the porosity and the fluid velocity and bends the fluid flow path.[43,44] Fig. 3(b) shows the microstructure of the SEM about the sodium-based bentonite permeated with GX bauxite leachates with a higher ionic strength of 224.5 mM. The montmorillonite mineral layer in the bentonite could occur smaller osmotic expansion, which result larger hydraulic conductivity under GX bauxite leachates. As the increase of ionic strength and decrease of swell index, smaller osmotic expansion and larger porosity occurred. Similarly, Fig. 3(c) shows the microstructure of SEM about the sodium-based bentonite permeated with SD bauxite leachates with a highest ionic strength of 620.3 mM. It could be clearly seen that the microstructure of bentonite has undergone more obvious porosity and the time of breakthrough Cr/Pb increased sharply.

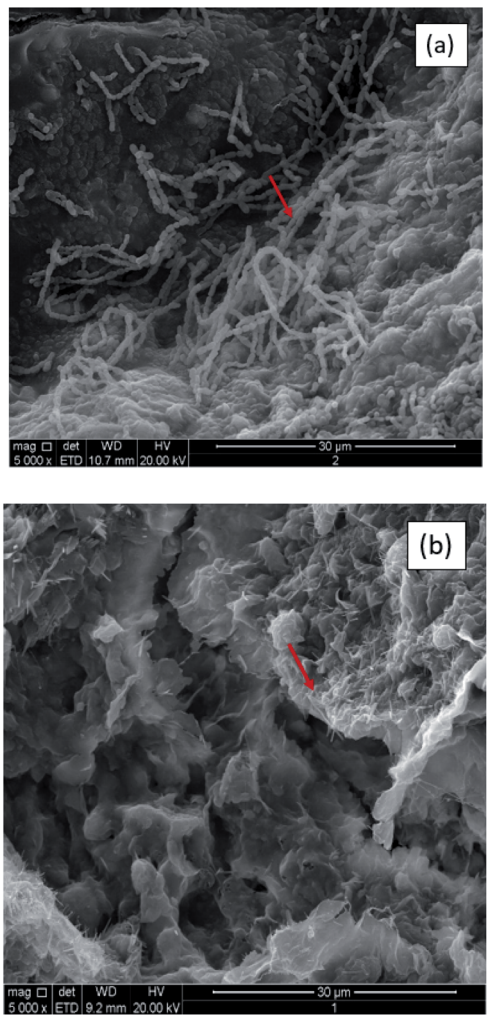

Fig. 4 SEM images of bentonite–polymer from BPC GCLs in DI water: (a) linear polymer structure (CP6.5) and (b) crosslinked polymer structure (CP7.5).

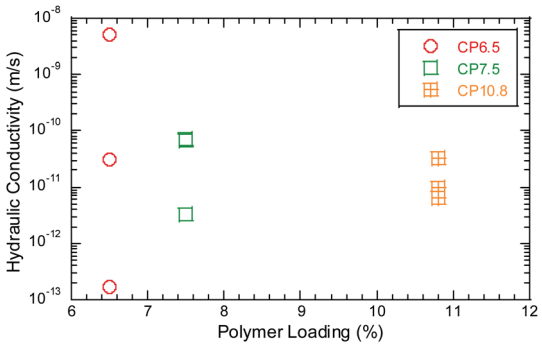

Fig. 5 Hydraulic conductivity of BPC GCLs as a function of polymer loading.

3.3 Effect of polymer in BPC GCLs on attenuation of Cr/Pb

In order to reduce porosity caused by the expansion of bentonite, the polymer was introduced to form bentonite–polymer composite GCLs, which could form macromolecules which consist of straight or branched chains.[45] SEM images of the microstructure of BPC GCLs with linear (CP6.5) and crosslinked-network structures (CP7.5) are shown in Fig. 4. The linear polymer has a covalently bonded collection of atoms that form a long "chain" and a curled state in Fig. 4(a), whereas the crosslinked polymer network structure has covalent bonds between chains that form a three-dimensional (3-D) network structure in Fig. 4(b).[38] Both structures could form a gel by binding water molecules with hydrophilic functional groups, which fills pores between bentonite granules and coats the surface of the bentonite.[37]

Enough polymer could block the pore spaces between the bentonite granules and retard attenuation of heavy metals by suppressing osmotic expansion of bentonite.[37] Hydraulic conductivity of the BPC GCLs to the bauxite liquors is shown in Fig. 5 as a function of polymer loading. With more polymer, the porosity will be correspondingly smaller and the rate of attenuation of heavy metals will be slower. For example, the polymer loading for the BPC GCLs increases from approximately 6.5%, 7.5% to 10.8%, the hydraulic conductivity is 5.0×10^{-9} m s^{-1}, to 6.7×10^{-11} m s^{-1} and 6.6×10^{-12} m s^{-1} for SD bauxite leachates with higher ionic strength. The time of breakthrough Cr increased from 1500 mL to 1800 mL and 1900 mL with increasing polymer loading.

With polymer elution occurring, the attenuation of heavy metals increased and the breakthrough occurred. Polymer elution indicated the pore spaces opened up and heavy metals eluted. At the same time, the concentration of leachates increases, the more polymer flows out with time, and the shorter the time for heavy metal breakthrough. For example, the time of breakthrough Cr/Pb were earlier for SD bauxite leachates with higher ionic strength than GX bauxite leachates. These finding showed that polymer content was necessary to block the pore spaces and maintain the content of heavy metals in bauxite leachates.

4. Conclusions

In this study, bauxite leachates in two typical aluminum industry was used to evaluate the effectiveness of GCL materials containing granular sodium bentonite (NaB) and bentonite polymer composite (BPC) GCLs on the attenuation of heavy metals. Based on the findings of this study, the following conclusions and recommendations are drawn:

(1) The BPC GCLs had hydraulic conductivities to bauxite leachates ranging from 10^{-8} to 10^{-12} m s^{-1}, and the concentrations of Cr (Pb) in the SD and GX bauxite leachates are 5.9 (1.1) and 0.1 (0.3) mg L^{-1}, respectively. Meanwhile, the BPC GCLs with a low hydraulic conductivity ($k < 10^{-10}$ m s^{-1}) retard the migration of Cr and Pb and the breakthroughs of Cr and Pb were not evident for the BPC GCLs with low hydraulic conductivities ($k < 10^{-10}$ m s^{-1}). After a long period of testing (cumulative flow > 2000 mL or >20 PVFs), the breakthrough of Cr and Pb in the test of low hydraulic conductivity (<10^{-10} m s^{-1}) becomes obvious and the maximum C_{Cr}/C_{Cro} reaches approximately 1. The Cr had a higher mobility than Pb in the BPC GCLs.

(2) The attenuation of heavy metals in bauxite leachates depends on the chemical properties of the liquor, the adsorption and osmotic expansion of bentonite, the polymer content and microstructure. Higher attenuation of heavy metals was obtained with bauxite leachates having higher ionic strength. The time of breakthrough Cr increased from 1500 mL to 2380 mL with increasing the swell index in SD and GX bauxite leachates. Similarly, the time of breakthrough Pb was earlier for SD bauxite leachates with higher ionic strength than GX bauxite leachates.

(3) Sufficient polymer content is needed to ensure BPC GCLs have adequately low hydraulic conductivity to suppress attenuation of heavy metals. The gelatinous structure associated with hydrated linear or crosslinked polymer diminishes when the polymer in a BPC is contacted by bauxite leachates. Compromising the hydrogel structure promotes polymer elution and leaves pore space open, resulting in attenuation of heavy metals. The polymer loading for the BPC GCLs increases from approximately 6.5%, 7.5% to 10.8%, the hydraulic conductivity is 5.0×10^{-9} m s^{-1}, to 6.7×10^{-11} m s^{-1} and 6.6×10^{-12} m s^{-1} for SD bauxite leachates with higher ionic strength. The time of breakthrough Cr increased from 1500 mL to 1800 mL and 1900 mL with increasing polymer loading.

Conflicts of interest

There are no conflicts to declare.

Acknowledgements

This research was funded by the Sichuan Science and Technology Program (No. 2019YJ0244), provided the financial support for this study. Sampling of red mud samples was supported by the National Natural Science Foundation of China and the Foundation of Key Laboratory of Soft Soils and Geoenvironmental Engineering (Zhejiang University).

Notes and references

1 M. Kishida, T. Harato, C. Tokoro and S. Owada, *Hydrometallurgy*, 2017, **170**, 58–67.

2 S. Xue, X. Kong, F. Zhu, W. Hartley, X. Li and Y. Li, *Environ. Sci. Pollut. Res.*, 2016, **23**(13), 12822–12834.
3 K. Evans, *J. Sustain. Metall.*, 2016, **2**(4), 316–331.
4 I. M. Nikbin, M. Aliaghazadeh, S. Charkhtab and A. Fathollahpour, *J. Cleaner Prod.*, 2018, **172**, 2683–2694.
5 Y. Su, Q. Zhu, J. Li, D. Wang, Z. Xing and L. Fang, *RSC Adv.*, 2019, **9**(18), 10305–10313.
6 C. Sun, J. Chen, K. Tian, D. Peng, X. Liao and X. Wu, *J. Environ. Res. Public Health*, 2019, **16**, 1297.
7 I. Burke, W. Mayes, C. Peacock, A. Brown, A. Jarvis and K. Gruiz, *Environ. Sci. Technol.*, 2012, **46**, 3085–3092.
8 W. Liu, X. Chen, W. Li, Y. Yu and K. Yan, *J. Cleaner Prod.*, 2014, **84**, 606–610.
9 Y. Du, M. Dai, J. Cao and C. Peng, *RSC Adv.*, 2019, **9**(57), 33486–33496.
10 D. A. Rubinos, G. Spagnoli and M. T. Barral, *J. Environ. Sci. Technol.*, 2016, **13**, 773–792.
11 I. Ghosh, S. Guha, R. Balasubramaniam and A. V. R. Kumar, *J. Hazard. Mater.*, 2011, **185**, 662–668.
12 J. Zhang, S. Liu, Z. Yao, S. Wu, H. Jiang, M. Liang and Y. Qiao, *Constr. Build. Mater.*, 2018, **180**, 605–613.
13 W. Shin and Y. K. Kim, *J. Soils Sediments*, 2016, **16**(2), 726–735.
14 D. Dodoo-Arhin, R. A. Nuamah, B. Agyei-Tuffour, D. O. Obada and A. Yaya, *Case Stud. Constr. Mater.*, 2017, **7**, 45–55.
15 C. Athanassopoulos, C. Benson, J. Chen and M. Donovan, *Geosynthetics*, IFAI, St. Paul, MN, 2015, pp. 181–186.
16 C. Benson, A. Oren and W. Gates, *Geotext. Geomembr.*, 2010, **28**(2), 206–218.
17 J. Scalia and C. Benson, *J. Geotech. Geoenviron. Eng.*, 2011, **137**, 1–13.
18 K. Tian, C. Benson and W. Likos, *J. Geotech. Geoenviron. Eng.*, 2016, **142**, 1–12.
19 H. Jo, T. Katsumi, C. Benson and T. Edil, *J. Geotech. Geoenviron. Eng.*, 2001, **127**(7), 557–567.
20 J. Chen, S. Bradshaw, C. Benson, J. Tinjum and T. Edil, *GeoCongress 2012 State of the Art and Practice in Geotechnical Engineering*, 2012, pp. 3729–3738.
21 G. Di Emidio, W. Van Impe and V. Flores, *GeoFrontiers 2011*, ASCE, Reston, VA, USA, 2011, pp. 1931–1940.
22 H. Jo, T. Katsumi, C. Benson and T. Edil, *J. Geotech. Geoenviron. Eng.*, 2001, **127**(7), 557–567.
23 M. Setz, K. Tian, C. Benson and S. Bradshaw, *Geotext. Geomembr.*, 2017, **45**(6), 665–673.
24 K. Norrish and J. Quirk, *Nature*, 1954, **173**(4397), 255–256.
25 M. Onikata, M. Kondo, N. Hayashi and S. Yamanaka, *Clays Clay Miner.*, 1999, **47**(5), 672–677.
26 K. Lange, R. K. Rowe and H. Jamieson, *Proceedings of the GeoQuebec 2004 (October) Conference Quebec*, 2004.
27 H. Ozhan, *Appl. Clay Sci.*, 2018, **161**, 364–373.
28 J. Chen, H. Salihoglu, C. Benson, W. J. Likos and T. B. Edil, *J. Geotech. Geoenviron. Eng.*, 2019, **145**(9), 04019038.
29 M. H. A. Rehim, A. M. Youssef and H. A. Essawy, *Mater. Chem. Phys.*, 2010, **119**(3), 546–552.
30 A. M. Youssef, F. M. Malhat, A. A. Abdel Hakim and I. Dekany, *Arabian J. Chem.*, 2017, **10**(5), 631–642.
31 M. A. Abd El-Ghaffar, A. M. Youssef and A. A. Abdel Hakim, *Arabian J. Chem.*, 2015, **8**(6), 771–779.
32 A. Fehervari, W. Gates, T. Turney, A. Patti and A. Bouazza, *Appl. Clay Sci.*, 2016, **134**, 2–12.
33 W. Gates, U. Shaheen, T. Turney and A. Patti, *Appl. Clay Sci.*, 2016, **124**, 94–101.
34 L. Y. Li and F. Li, *J. Environ. Eng.*, 2001, **127**(5), 420–429.
35 P. Yang, T. Jiang, Y. Zhang and Z. Li, *Adv. Civ. Eng.*, 2018, (Pt 9), 1–9.
36 K. Lange, R. K. Rowe and H. Jamieson, *Geotech. Spec. Publ.*, 2005, **16**(130), 11–27.
37 K. Tian and C. Benson, *Proceedings of the 8th International Congress on Environmental Geotechnics*, 2019, vol. 2, pp. 672–678.
38 M. Mendes, N. Touze-Foltz, E. Palmeira and P. Pierson, *Geosynth. Int.*, 2010, **17**(1), 34–47.
39 J. Scalia, C. Benson, G. Bohnhoff, T. Edil and C. Shackelford, *J. Geotech. Geoenviron. Eng.*, 2014, **04013025**, 1–13.
40 H. Jo, C. Benson, J. Lee, C. Shackelford and T. Edil, *J. Geotech. Geoenviron. Eng.*, 2005, **131**(4), 405–417.
41 M. Hosney and K. Rowe, *Environmen. Geotech.*, 2019, **6**(3), 155–161.
42 C. Shackelford, C. Benson, T. Katsumi, T. Edil and L. Lin, *Geotext. Geomembr.*, 2000, **18**(2–4), 133–162.
43 J. Lee and C. Shackelford, *J. Geotech. Geoenviron. Eng.*, 2005, **131**(1), 64–77.
44 S. Bradshaw and C. Benson, *J. Geotech. Geoenviron. Eng.*, 2014, **140**(4), 04013038.
45 S. Ray and M. Okamoto, *Prog. Polym. Sci.*, 2003, **28**(11), 1539–1641.

